Theoretical and Applied Mechanics Letters xxx (xxxx) xxx

Contents lists available at ScienceDirect

Theoretical and Applied Mechanics Letters

journal homepage: www.elsevier.com/locate/taml

Numerical optimisation of a classical stochastic system for targeted energy transfer

Oleg Gaidai [a], Yubin Gu [b,*], Yihan Xing [d], Junlei Wang [e], Daniil Yurchenko [c]

[a] Shanghai Engineering Research Center of Marine Renewable Energy, Shanghai Ocean University, China
[b] School of Mechanical and Electrical Engineering, Guilin University of Electronic Technology, China
[c] Institute for Sound and Vibration Research, University of Southampton, UK
[d] Department of Machine, Building and Materials Technology, University of Stavanger, Norway
[e] School of Mechanical and Power Engineering, Zhengzhou University, China

A R T I C L E I N F O

Article history:
Received 6 November 2022
Revised 12 December 2022
Accepted 14 December 2022
Available online xxx

Keywords:
Targeted energy transfer
Surrogate optimisation
Stochastic system
Random vibration

A B S T R A C T

The paper studies stochastic dynamics of a two-degree-of-freedom system, where a primary linear system is connected to a nonlinear energy sink with cubic stiffness nonlinearity and viscous damping. While the primary mass is subjected to a zero-mean Gaussian white noise excitation, the main objective of this study is to maximise the efficiency of the targeted energy transfer in the system. A surrogate optimisation algorithm is proposed for this purpose and adopted for the stochastic framework. The optimisations are conducted separately for the nonlinear stiffness coefficient alone as well as for both the nonlinear stiffness and damping coefficients together. Three different optimisation cost functions, based on either energy of the system's components or the dissipated energy, are considered. The results demonstrate some clear trends in values of the nonlinear energy sink coefficients and show the effect of different cost functions on the optimal values of the nonlinear system's coefficients.

Targeted Energy Transfer (TET) phenomenon has been attracting attention of researchers worldwide in last 20 years, focusing on the essence of the irreversible energy transfer between linear and nonlinear elements in nonlinear systems. TET can be used for effective vibration mitigation, energy harvesting and in other relevant applications [1–5], thus it can be encountered in mechanical, electrical and biological systems on both macro- and micro-levels. In recent years the TET phenomenon has been extensively studied on an exemplary two-degree-of-freedom systems, where a primary linear oscillator (LO), under a deterministic excitation, was connected by a nonlinear (cubic) spring to a secondary system, which is often called as a Nonlinear Energy Sink (NES). Typically, the aim of introducing the secondary mass is to mitigate vibrations of the LO by transferring and dissipating its energy. This reasonably simple nonlinear setup, however, cannot be treated analytically exactly, thus it has to be studied either using approximately analytical methods or numerically. Treating the system as weakly-nonlinear [6,7] have shown that TET can be effective in vicinity of 1:1 resonance depending on the values of the mass ratio and damping coefficient. However, recent study [8] have revealed that a combination of a linear and nonlinear springs of the coupled secondary system can also be very effective over a wide range of excitation parameters in the free vibration problem. Application of approximate methods, although provides some insight into the fundamentals of TET, cannot reveal its properties in full due to obvious limitations of these methods, which require the system's parameters to be small, i.e. $O(\varepsilon)$. Perhaps, the only well-known class of nonlinear systems that can be treated exactly analytically is vibroimpact systems with inelastic instantaneous impacts. In Refs. [9–14] the authors treated this system using approximate analytical, numerical and experimental approaches. Most recent developments in TETs can be found in seminal review paper [15].

Stochastic TET systems has been studied much less, than their deterministic counterparts. In Ref. [16] the authors have shown that for a weakly coupled system the deterministic regime of energy transfer is preserved, when the excitation is Gaussian and additive. In Ref. [17] the authors used complexification averaging approach to treat the system analytically and an efficiency of the NES as a function of its parameters and noise intensity was demon-

* Corresponding author.
E-mail address: gyb13912193900@gmail.com (Y. Gu).

https://doi.org/10.1016/j.taml.2022.100422

strated. In particular it was shown that for low values of noise intensities energy transfer was not very efficient. At high values of the noise intensity, where the approximate solution may not work, the energy transfer and dissipation through the nonlinear system was more effective, but it was not growing linearly, for example, with increasing mass ratio. Another interesting observation made in Ref. [17] was regarding the NES's damping coefficient, which increasing values improved nonlinearly the NES's dissipation performance. These observations have motivated the authors of this paper to study the optimal performance of such a system when both NES's parameters, its stiffness and damping coefficients, are optimised through a numerical optimisation algorithm. To implement the optimisation algorithm the problem is addressed numerically, which also removes the limitations on the system's parameters values, which otherwise have to be small for an approximate analytical treatment.

To study the TET mechanism, the classical two-degree-of-freedom system a with cubic nonlinearity is considered:

$$\begin{aligned} m_1\ddot{x}_1 + k_1x_1 + c_1\dot{x}_1 + c_2(\dot{x}_1-\dot{x}_2) + \alpha_1(x_1-x_2)^3 &= \sigma_1\zeta(t), \\ m_2\ddot{x}_2 - c_2(\dot{x}_1-\dot{x}_2) - \alpha_1(x_1-x_2)^3 &= 0. \end{aligned} \tag{1}$$

where m_1, m_2 are the primary and secondary masses, x_1, x_2 are the corresponding displacements from the equilibrium positions, k_1 is the linear stiffness coefficient of the linear oscillator, α_1 is the cubic stiffness coefficients of the nonlinear spring connecting the LO and the NES, and c_1, c_2 are the viscous damping (friction) coefficients, $\zeta(t)$ is a zero-mean Gaussian white noise and σ_1^2 is the noise intensity. Following Ref. [17] one can introduce a new set of parameters, $\epsilon = m_2/m_1$, $\Omega^2 = k_1/m_1$, $\sigma = \sigma_1/m_1$, $\lambda_1 = c_1/m_1$, $\lambda_2 = c_2/m_1$ and $\lambda_3 = \alpha/m_1$, so that Eq. (1) can be rewritten as:

$$\begin{aligned} \ddot{x}_1 + \Omega^2x_1 + \lambda_1\dot{x}_1 + \lambda_2(\dot{x}_1-\dot{x}_2) + \lambda_3(x_1-x_2)^3 &= \sigma\zeta(t), \\ \epsilon\ddot{x}_2 - \lambda_2(\dot{x}_1-\dot{x}_2) - \lambda_3(x_1-x_2)^3 &= 0. \end{aligned} \tag{2}$$

The main goal of this study is to find the optimal values of the stiffness and damping coefficients of the NES and establish an empirical relationship with the noise intensity. To implement this effectively an optimisation algorithm should be used, which will deliver an extremum to a selected cost function. The choice of the latter is not unique and thus a number of cost functions will be used, so that the efficacy of the NES can be compared.

To use the optimisation algorithm and explore non-small nonlinearity cases (large values of noise intensity, mass ratio, etc.) the problem is treated numerically. The surrogate optimisation approach is used to optimise the TET in Eq. (2) by selecting the best possible values of the nonlinear system parameters depending on the values of other given parameters and noise intensity. The surrogate optimisation provides an attractive numerical approach based on simple interpolation or regression models built from objective function values at a limited number of sample points and update these models iteratively. These approximate objective function are called surrogates. The surrogate optimisation is a powerful alternative to the gradient-based methods, which may bring the system to a local extrema instead of the global one. Moreover, due to the surrogate optimisation algorithm, it is often used when the cost function evaluation is expensive or complicated, like in stochastic systems, for instance. The optimisation algorithm searches for a global extremum and alternates between two phases: the phase of generating or updating a surrogate and the phase of performing global optimisation via the current surrogate. The stopping criterion is usually specified just by limiting the number of iterations or objective function evaluations. Since system of Eq. (2) is stochastic, it is required to have either long enough time series or very representative sample of the response to collect its statistical properties for a given set of the system's parameters and the excitation. The resulting dependence of the parameters of the nonlinear system on the noise intensity and values of other parameters can be approximated via an interpolation or regression technique. We propose to use Kriging [18] (which is a form of Gaussian process regression) for that purpose.

In other words the adapted algorithm of surrogate optimisation for this problem has the following steps [19,20]:

1. Construct a quasi-random initial grid in the bounded space of parameters to be optimised. The grid is constructed from a limited number of quasi–Monte Carlo nodes using Latin Hypercube sampling algorithm [21]. In general, quasi–Monte Carlo grids reduce the clamping of standard Monte Carlo grids, which is critical to high-dimensional problems, and can rely on Halton, Sobol, or Faure quasi-random number sequences [22,23].;
2. Evaluate the cost function at the current grid nodes in the parameters space. This is performed by numerically integrating the differential Eq. (2) using the Monte-Carlo simulations and Runge-Kutta algorithm with the time step $\Delta t = 0.01$. Since the process is random, a relatively long time interval is selected (around $10^5 T_n$, where T_n was the natural period of the LO. This procedure executed 20 times, generating each time a different random excitation sequence, to obtained a mean value of the cost function at the node;
3. Construct a quickly computable surrogate approximation of the cost function based on the grid data;
4. Solve an auxiliary optimisation problem for the surrogate approximation and include the obtained solution in the grid;
5. Evaluate the original cost function at the new grid point, as explained in step 2 above, and update the best solution in case of improvement;
6. Trace if the maximum number of cost function evaluations is reached, which was set to 50 in this study. If not repeat from step 2, otherwise stop.

It should be noted that although there are some results on convergence of the built surrogate to the true cost function with increasing number of node, it is hard and expensive to estimate the maximum error numerically. The reason is that the surrogate provides a good and fast-computed estimation of the cost function, which is very expensive to calculate by the classical methods. The values of the surrogate coincide with the cost function values at the nodes only, therefore to calculate an error it is required to calculate the surrogate and the true cost function within the entire space of parameters.

When the damping coefficient λ_2 is given in advance, the stiffness coefficient value λ_3 can be optimised according to a selected cost function. The cost function significantly influences the outcome of the optimisation, thus it should be carefully chosen. Moreover, the cost function of a single parameter (for instance for λ_3), optimisation may differ from the results obtained in two parameters optimisation (λ_2 and λ_3), thus these two cases are considered separately in the following paragraph. The values of the other constant parameters are taken similar to Ref. [17], namely, $\Omega^2 = 1$, $\lambda_1 = \lambda_2 = 0.005$. To implement the optimisation approach one can choose to maximise the following measure, defined as:

$$\max_{\lambda_3\in[0,\lambda_{3R}]} \eta_d, \qquad \eta_d = \frac{\frac{\lambda_2}{T}\int_0^T(\dot{x}_1(t)-\dot{x}_2(t))^2\,dt}{<E_T>}\cdot 100\%, \tag{3}$$

where λ_{3R} is the specified top bound of the nonlinear stiffness parameter λ_3, $<E_T>$ is the averaged total energy of the system

$$<E_T> = \frac{1}{2}<\dot{x}_1^2> + \frac{\epsilon}{2}<\dot{x}_2^2> + \frac{\Omega^2}{2}<x_1^2> + \frac{\lambda_3}{4}<(x_1-x_2)^4> \tag{4}$$

and T is a sufficiently large time horizon to capture the statistics of the excitation and response. The top of this fraction is the amount of energy dissipated by the secondary system, which should be maximised. It can be seen that this function reaches maximum when the difference between the velocities is maximal, which obviously occurs when both the masses oscillate in anti-phase, i.e. when $x_1(t)$ and $x_2(t)$ have different signs. It should be noted that when the damping coefficient is also optimised this measure may not be very suitable since it is proportional to the damping coefficient and it may lead to a trivial result of the largest damping coefficient value out of the given interval.

Another useful measure is the amount of averaged kinetic energy left in the LO, which has to be minimised:

$$\min_{\lambda_3\in[0,\lambda_{3R}]} \eta_{kp}, \quad \eta_{kp} = \frac{\frac{1}{2}<\dot{x}_1^2>}{<E_T>} \cdot 100\%, \tag{5}$$

However, this measure does not show whether the energy is dissipated or simply stored in the secondary system. The third option is to maximise the amount of kinetic energy in the secondary system:

$$\max_{\lambda_3\in[0,\lambda_{3R}]} \eta_{ks}, \quad \eta_{ks} = \max_{\lambda_3} \frac{\frac{\epsilon}{2}<\dot{x}_2^2>}{<E_T>} \cdot 100\%, \tag{6}$$

The limitation of this measure is that the optimisation algorithm will try to find the nonlinear stiffness coefficient such that the energy is transferred to the secondary system rather than being dissipated, when the damping coefficient λ_2 is fixed. When λ_2 is an optimisation parameter, it would be reasonable to expect that it could be as small as possible to keep a high energy level of NES. Although in this paper the above optimisation criteria are used separately to identify the fundamental trends and features f the stochastic system, it is possible to combine them to potentially achieve a better result.

Figure 1 demonstrates the results of λ_3 optimisation for different values of ϵ and noise intensity σ. The left column represents the optimal values of λ_3 coefficient according to the selected criteria, whereas the right column represents the measures described by Eqs. (3), (5) and (6). The presented patterns in the left column of Fig. 1 are similar, the higher the noise intensity values the lower the values of λ_3, which provide maximum to the corresponding measure. It should be noted that the nonlinear decaying trend can be accurately approximated by $\approx C/\sigma^2$ curve, where C is a constant. The effect of increasing ϵ can also be seen comparing the curves in the same plots, where the values of optimal λ_3 grow up with increasing ϵ. This result agrees with observations reported in Ref. [17] where basically the authors showed that increase in ϵ may be beneficial to some extend for a given value of the system parameters and noise intensity. One can also see that the values of λ_3 obtained based on η_{kp} and η_{ks} are always higher than those obtained for optimal η_d value. However, carefully assessing the results presented in the right column one can make two important observations. Firstly, for a given value of ϵ the extreme values of the measures are independent of noise intensity σ^2. This is a very interesting and counter-intuitive result, since one would expect higher value of these measures at higher values of noise intensity. Practically, this result indicates that the NES of the stochastic system with a particular set of parameters can absorbed and damped a certain maximum amount of energy. Secondly, the behaviour of all three measures is different, as can be seen in Fig. 2, where the values of η_{kp}, η_{ks} and η_d have been plotted as a function of ϵ for $\sigma = 0.01$, although, as we know now from the above observation, it does not matter what value of σ is taken.

One can observe in Fig. 2 that η_d measure can reach its maximum value within the considered interval, fading out for increasing values of ϵ. It should be noted that measure Eq. (5) is just a half of the total energy, since the potential energy due to linear spring $(0.5\Omega^2 x_1^2)$ has not been used in Eq. (5). This measure takes its maximum value at very low values of ϵ and slowly decays with increasing ϵ, whereas η_{ks} demonstrates an opposite trend and grows with increasing ϵ. These curves indicate that to reach low energy of the primary system, ϵ should be large, which also leads to high energy of the NES, however, energy losses in this case will be small, at least when the viscous damping is used.

Table 1
Validation of optimal results for $\epsilon = 0.3$ and $\sigma = 0.3$, where * indicate the optimal values according to Eq. (6).

λ_3	0.005	0.02*	0.1	0.5	1.0	10
$< E_{NES} >$	0.5082	1.022	1.3882	1.4091	1.3614	1.3506
$< E_T >$	2.8470	3.5123	6.0716	7.8554	8.0926	9.5086
$\eta_{ks}(\%)$	17.8496	29.0982	22.8642	17.9386	16.8254	14.2037

The obtained numerical results, presented in Fig. 1, have been validated by taken some non-optimal values of λ_3 and calculating the total and the NES energies. These results are presented in Table 1. The value $\lambda_3 = 0.02$ is the optimal according to criteria as Eq. (6), and with this value the energy of NES reaches 29%, demonstrating its relatively high efficiency. It can also be seen that the total energy of the system grows with increasing value of λ_3, whereas the NES energy demonstrates a negative parabolic trend.

The time history of the LO and NES for $\lambda_3 = 0.02$ and $\lambda_3 = 1.0$ are presented in Fig. 3a and 3b respectively. Lower response amplitude of the LO (x_1) and high response amplitude of the NES (x_2) can be clearly seen in these figures for the optimal value of λ_3. This demonstrates the effectiveness of the proposed optimisation algorithm in selecting the optimal parameters of NES. Plots in Fig. 3c and 3d demonstrate the time history of the response for the optimal values of λ_3 based on measure Eqs. (3) and (5) correspondingly. It should be noted, that due to the stochastic nature of the problem, the algorithm proposes the optimal values of the parameters based on averaged values, practically relying on stationary properties of the response, which may not be the case when the noise sample is too short or not very representative. Thus, a very representative noise sample is essential for perfect selection of the parameters, which is not computationally expensive due to the features of the surrogate optimisation algorithm combined with Latin Hypercube sampling.

In Ref. [17] the authors claimed that for very small values of noise intensity the NES was not effective. Figure 4 demonstrates the results for $\sigma = 0.005$, $\epsilon = 0.05$ and two values of the NES's stiffness coefficient: the optimal value $\lambda_3 = 10.43$, provided by the optimisation algorithm and non-optimal optimal one, e.g. $\lambda_3 = 1.0$. These values are very similar to those selected in Ref. [17]. Figure 4a clearly demonstrate the fact that with very small values of noise intensity $(\sigma << 1)$ the NES can still be effective as long as its parameters have been optimised. In the optimal case the efficiency reaches $\eta_{ks} = 15.94\%$, which may not be as high as in some other above mentioned cases, whereas $\eta_{ks} = 0.35\%$ when $\lambda_3 = 1.0$, as shown in Fig. 4b, where the NES is highly inefficient. The optimal λ_3 value can be further improved by tuning λ_2 and ϵ values. This clearly demonstrates the need for optimising the system's parameters based on the noise intensity and show that at low values of noise intensity the NES can be effective.

It should be mentioned that when the NES's viscous damping coefficient is increased the optimal values of λ_3 are also affected. Figure 5 presents the optimal values of λ_3, shown in red, as a function of λ_2. Figure 5a demonstrates the optimal λ_3 values and the corresponding peaks of η_{ks}, indicating that the NES energy is being reduced with increasing value of NES's damping coefficient λ_2. Figure 5b demonstrates the optimal λ_3 and the corresponding η_d values, where the latter grows initially, reaching its peak value, and then dropping down with further increase of λ_2. It is also observed by comparing Fig. 5a and 5b that optimal values of λ_3 are higher

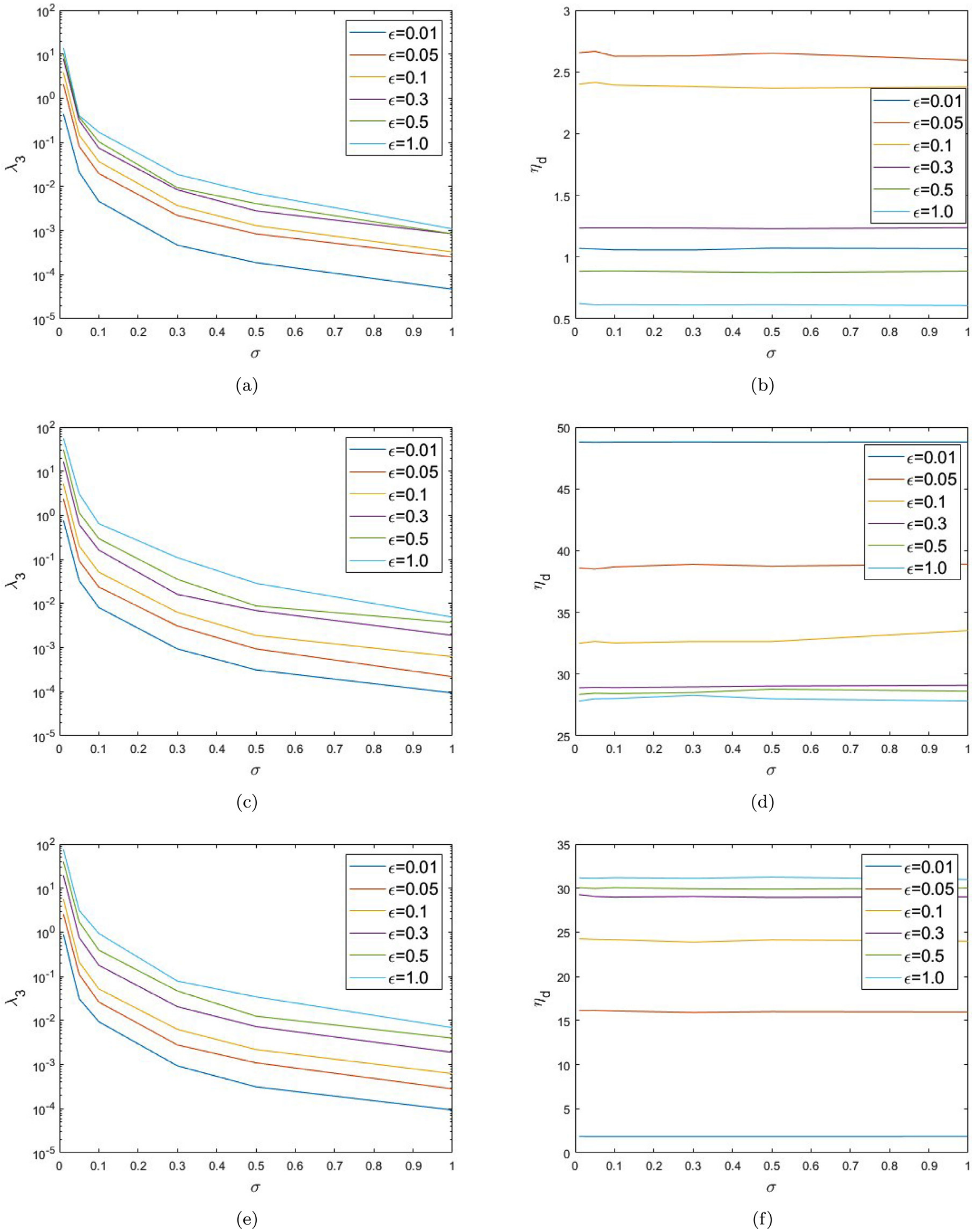

Fig. 1. Optimal values of λ_3 in log format (left column) and the corresponding measure (right column) for η_d (**a,b**), η_{kp} (**c,d**) and η_{ks} (**e,f**).

for η_{ks} than that for η_d. Thus, to achieve the maximum energy dissipation via the NES the viscous damping coefficient does not have to be as high as possible, as could be intuitively expected, but it rather has to be properly tuned based on the values of the system's parameters.

Table 2 presents the results of two-parameter optimisation based on η_d measure. In this case the damping coefficient of the NES λ_2 is optimised together with the stiffness coefficient λ_3, keeping the rest of the coefficients as above. It can be seen that λ_2 values have been relatively identical, close to 0.02 value, as well as the extreme values of η_d, however, the values of λ_3 were going down with increasing noise intensity values. Values of two other measures are also presented in the table and they are relatively the same over the range of considered σ values. These results also indicate that the optimal λ_2 remains the same for different values of the noise intensity.

The paper studies numerically the targeted energy transfer mechanism in a classical two-degree-of-freedom system consisting of the linear oscillator (LO) and the nonlinear energy sink (NES) connected to the LO by a cubic spring. To achieve the maxi-

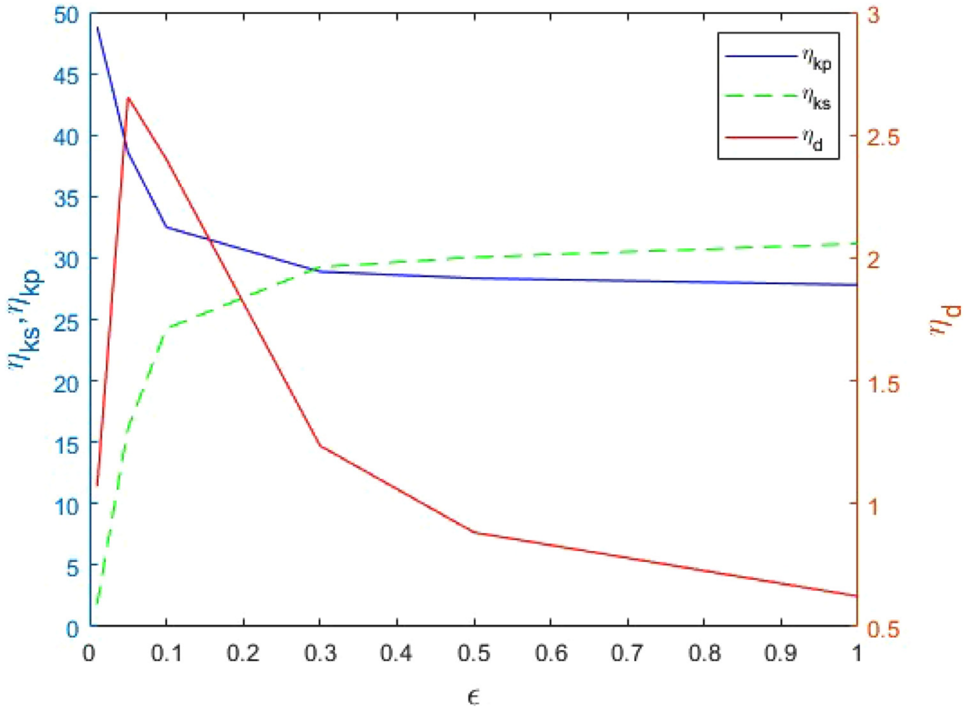

Fig. 2. The extreme values of η_{kp}, η_{ks} and η_d obtained for $\sigma = 0.3$.

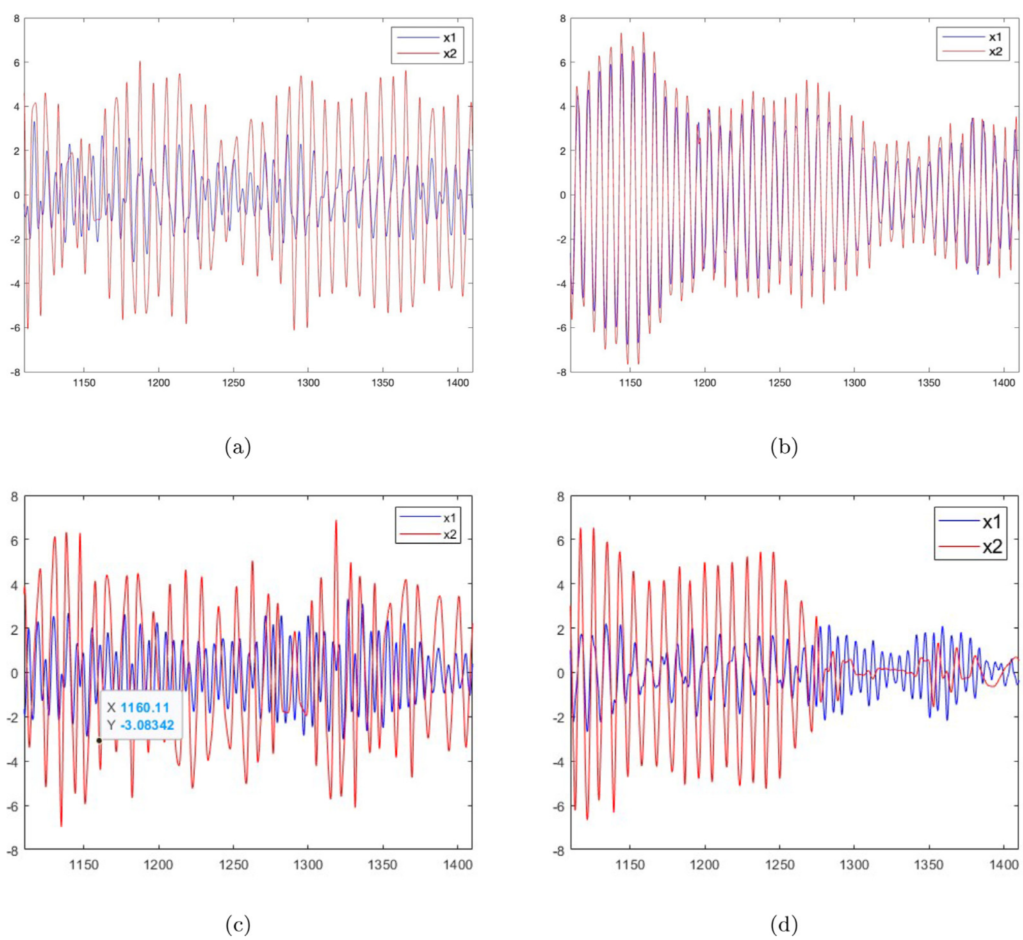

Fig. 3. Time response of the primary mass and NES for values for $\sigma = 0.3$ and $\epsilon = 0.3$ with (**a**) optimal $\lambda_3 = 0.02$ based on Eq. (6), (**b**) non-optimal $\lambda_3 = 1.0$, (**c**) optimal value $\lambda_3 = 8.4 \times 10^{-3}$ based on Eq. (3) and (**d**) optimal value $\lambda_3 = 0.0161$ based on Eq. (5).

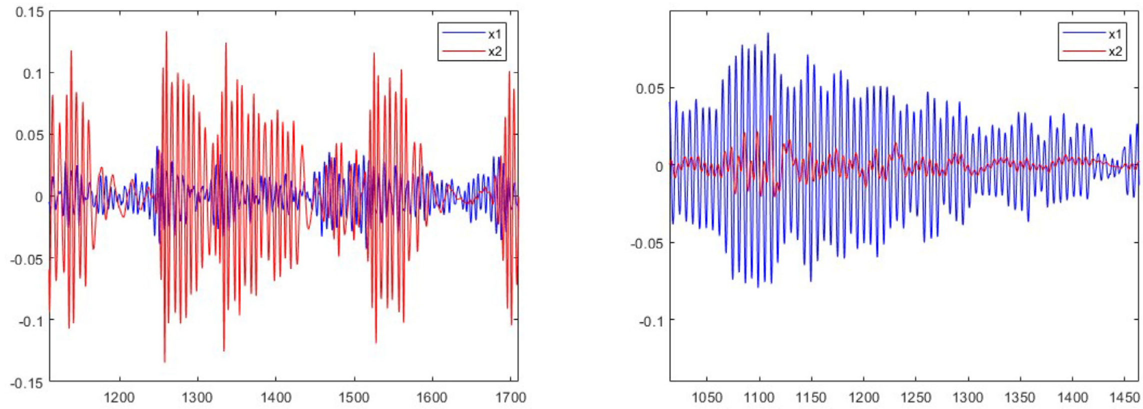

(a) (b)

Fig. 4. Time response of the primary mass and NES with optimal $\lambda_3 = 10.43$ (**a**) and non-optimal $\lambda_3 = 1.0$ (**b**) values for $\sigma = 0.005$ and $\epsilon = 0.05$.

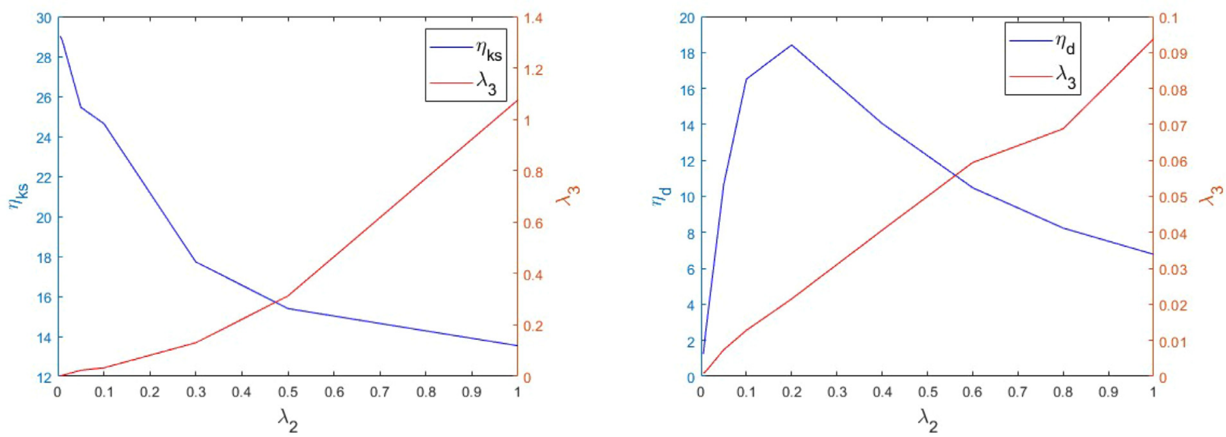

(a) (b)

Fig. 5. The optimal values of λ_3 based on measures from Eq. (6) (**a**) and Eq. (4) (**b**), correspondingly for $\sigma = 1.0$ and $\epsilon = 0.3$.

Table 2
Two-parameter (λ_2 and λ_3) optimisation according to Eq. (3) for $\epsilon = 0.3$ and different values of σ.

σ	λ_3	λ_2	η_d(%)	η_{kp}(%)	η_{ks}(%)
0.01	242.03	0.0208	18.448	38.7845	13.1245
0.1	2.359	0.0211	18.419	39.1321	12.7281
0.3	0.2596	0.0213	18.456	39.0794	12.724
1.0	0.0215	0.0205	18.427	39.7639	12.9824

mum targeted energy transfer efficiency of the NES, its parameters are optimised by implementing a surrogate optimisation algorithm. This algorithm is based on a machine-learning procedure of building a surrogate objective function and finding an optimal set of parameters according to a selected cost function. Three different cost functions have been considered and implemented to obtain the optimal values of the nonlinear stiffness λ_3 and damping λ_2 coefficients for one- and two- parameter optimisation procedure. The other system's parameters were kept constant, with values similar to Ref. [17], whereas the mass ratio ϵ and the noise intensity σ were varied.

It has been established that for a given value of ϵ and increasing values of σ the optimal values of the nonlinear stiffness coefficient λ_3 decreases as $\approx 1/\sigma^2$. It has been also shown that the extreme values of the measure, proposed in this work, has been independent of the noise intensity. For a given value of noise intensity, the optimal λ_3 values have demonstrated different trends for the three considered measures. Namely, with increasing values of mass ratio ϵ, the mean nondimensional energy of the primary system decays, whereas the mean nondimensional energy of NES increases. At the same time, the energy dissipated by the NES reaches its peak not at the end points of the interval. Thus, a reasonable NES efficiency can be achieved for small values of noise intensity, by adjusting the mass ratio coefficient ϵ and the damping coefficient λ_2 for a specific noise intensity value.

Thus, the NES's damping coefficient influence the optimal values of NES's stiffness coefficient, where the latter was increasing with increasing values of damping, thereby reducing the energy of the NES. Based on the obtained results, a relatively low values of the NES's damping coefficient can improve the energy losses as well as keep high energy level in the NES. One of the possible reason for this is the phase shift between the LO and the NES, which depends on λ_2 and should provide an anti-phase response.

The present work validates the proposed optimisation approach, proven to be reasonably accurate and computationally efficient. A mathematically strict error analysis cannot be effectively conducted, therefore the obtained results were validated by comparing to the results obtained by crude Monte-Carlo simulations with non-optimal values of the parameters. Despite some progress in the area of surrogate optimisation, further studies and developments are required to improve the algorithm for stochastic problems.

Declaration of Competing Interest

The authors declare that they have no known competing financial interests or personal relationships that could have appeared to influence the work reported in this paper.

Acknowledgements

The authors gratefully acknowledge partial funding for this work from NSF-CMMI 2009270 and EPSRC EP/V034391/1.

References

[1] Y. Fu, H. Ouyang, R. Davis, Nonlinear dynamics and triboelectric energy harvesting from a three-degree-of-freedom vibro-impact oscillator, Nonlinear Dyn. 92 (2018) 1985–2004.
[2] R.D. Jenkins, G.J. Daniels, D.L. Andrews, Quantum pathways for resonance energy transfer, J. Chem. Phys. 120 (2004) 11442–11448.
[3] Y.S. Lee, A.F. Vakakis, L.A. Bergman, et al., Suppression aeroelastic instability using broadband passive targeted energy transfers, part 1: theory, AIAA J. 45 (2007) 693–711.
[4] H. Li, A. Li, X. Kong, et al., Dynamics of an electromagnetic vibro-impact nonlinear energy sink, applications in energy harvesting and vibration absorption, Nonlinear Dyn 108 (2022) 1807–1819, doi:10.1007/s11071-022-07253-5.
[5] A.F. Vakakis, Inducing passive nonlinear energy sinks in vibrating systems, J. Vib. Acoust. 123 (2001) 324–332.
[6] E. Gourdon, C. Lamarque, Energy pumping with various nonlinear structures: numerical evidences, Nonlinear Dyn. 40 (2005) 281–307.
[7] H. Xiong, X. Kong, Z. Yang, et al., Response regimes of narrow-band stochastic excited linear oscillator coupled to nonlinear energy sink, Chin. J. Aeronaut. 28 (2015) 457–468.
[8] I. Yegorov (Egorov), A. Uden, D. Yurchenko, Optimal Performance Comparison of Nonlinear Energy Sinks and Linear Tuned Mass Dampers, International Design Engineering Technical Conferences and Computers and Information in Engineering Conference, volume 9: 17th International Conference on Multibody Systems, Nonlinear Dynamics, and Control (MSNDC), 2021.
[9] A. Afsharfard, Suppressing forced vibrations of structures using smart vibro-impact systems, Nonlinear Dyn. 83 (2016) 1643–1652.
[10] T. Li, S. Seguy, A. Berlioz, Dynamics of cubic and vibro-Impact nonlinear energy sink: analytical, numerical, and experimental analysis, J. Vib. Acoust. 138 (2016) 03101.
[11] T. Li, S. Seguy, A. Berlioz, Optimization mechanism of targeted energy transfer with vibro-impact energy sink under periodic and transient excitation, Nonlinear Dyn. 87 (2017) 2415–2433.
[12] G. Pennisi, C. Stéphan, G. Michon, Vibro-impact nes: A correlation between experimental investigation and analytical description, in: E. Wee Sit (Ed.), "Sensors and Instrumentation, Volume 5, Springer International Publishing, Cham, 2016, pp. 137–142.
[13] Y. Yan, Y. Liu, M. Liao, A comparative study of the vibro-impact capsule systems with one-sided and two-sided constraints, Nonlinear Dyn. 89 (2017) 1063–1087.
[14] B. Youssef, R. Leine, A complete set of design rules for a vibro-impact nes based on a multiple scales approximation of a nonlinear mode, J. Sound Vib. 501 (2021) 116043.
[15] A.F. Vakakis, O.V. Gendelman, L.A. Bergman, et al., Nonlinear targeted energy transfer: state of the art and new perspectives, Nonlinear Dyn 108 (2022) 711–741.
[16] T.P. Sapsis, A.F. Vakakis, L.A. Bergman, Effect of stochasticity on targeted energy transfer from a linear medium to a strongly nonlinear attachment, Probab. Eng. Mech. 26 (2011) 119–133.
[17] P. Kumar, S. Narayanan, S. Gupta, Targeted energy transfer in stochastically excited system with nonlinear energy sink, Eur. J. Appl. Math. 30 (2019) 869–886.
[18] C. Chilan, B. Conway, Optimal nonlinear control using hamilton–jacobi–bellman viscosity solutions on unstructured grids, J. Guid. Control Dyn. 43 (2019) 1–9.
[19] H.M. Gutmann, A radial basis function method for global optimization, J. Global Optim. 19 (1999) 2001.
[20] S. Koziel, L. Leifsson, Introduction to Surrogate Modeling and Surrogate-Based Optimization, Springer International Publishing, Cham, 2016, pp. 31–61.
[21] K.Q. Ye, W. Li, A. Sudjianto, Algorithmic construction of optimal symmetric latin hypercube designs, J. Stat. Plan Inference 90 (2000) 145–159.
[22] D. Jones, A taxonomy of global optimization methods based on response surfaces, J. Global Optim. 21 (2001) 345–383, doi:10.1023/A:1012771025575.
[23] L. Kocis, W.J. Whiten, Computational investigations of low-discrepancy sequences, ACM Trans. Math. Softw. 23 (1997) 266–294.